

Newcombe VF, Correia MM, Ledig C, Abate MG, Outtrim JG, Chatfield D, Geeraerts T, Manktelow AE, Garyfallidis E, Pickard JD, Sahakian BJ, Hutchinson PJ, Rueckert D, Coles JP, Williams GB, Menon DK. Dynamic Changes in White Matter Abnormalities Correlate With Late Improvement and Deterioration Following TBI: A Diffusion Tensor Imaging Study. *Neurorehabil Neural Repair*. 2016 Jan;30(1):49-62. doi: 10.1177/1545968315584004.

## Research Article

### **Dynamic changes in white matter abnormalities correlates with late improvement and deterioration following TBI: A diffusion tensor imaging study**

VFJ Newcombe MD PhD,<sup>1,2</sup> MM Correia PhD,<sup>3</sup> C Ledig PhD,<sup>4</sup> MG Abate MD,<sup>1,5</sup> JG Outtrim MSc,<sup>1</sup> D Chatfield BSc,<sup>1</sup> T Geeraerts MD PhD,<sup>1,6</sup> A Manktelow MSc,<sup>1</sup> E Garyfallidis PHD,<sup>7</sup> JD Pickard FMedSci,<sup>2,8</sup> BJ Sahakian FMedSci,<sup>9,10</sup> PJ Hutchinson MD PhD,<sup>8</sup> D Rueckert PhD,<sup>4</sup> JP Coles MD PhD,<sup>1,2</sup> GB Williams PhD,<sup>2</sup> DK Menon FMedSci.<sup>1,2</sup>

<sup>1</sup> University Division of Anaesthesia, School of Clinical Medicine, University of Cambridge, CB2 0QQ, UK.

<sup>2</sup> Wolfson Brain Imaging Centre, Department of Clinical Neurosciences, University of Cambridge, CB2 0QQ, UK.

<sup>3</sup> MRC Cognition and Brain Sciences Unit, University of Cambridge, CB2 7EF, UK.

<sup>4</sup> Department of Computing, Imperial College London, UK

<sup>5</sup> Neuroranimazione, Department of Perioperative Medicine and Intensive Care, San Gerardo Hospital, Monza, Milan, Italy

<sup>6</sup> Anesthesiology and Critical Care Department, University Hospital of Toulouse, University Toulouse 3 Paul Sabatier, Toulouse, France

<sup>7</sup> University of Sherbrooke, Computer Science Department, Sherbrooke, QC, Canada.

<sup>8</sup> Academic Neurosurgery Unit, Department of Clinical Neurosciences, University of Cambridge, CB2 0QQ, UK.

<sup>9</sup> 3, School of Clinical Medicine, University of Cambridge, CB2 2QQ UK

<sup>10</sup> MRC/Wellcome Trust Behavioural and Clinical Neuroscience Institute, University of Cambridge, CB2 3EB, UK

Corresponding author: Virginia Newcombe

Corresponding author's address: Division of Anaesthesia, Box 93,  
Addenbrooke's Hospital, Hills Road  
Cambridge, CB2 2QQ

Corresponding author's phone: +44 (0) 1223 274446 Fax: +44 (0) 1223 217887

Corresponding author's e-mail address: vfjn2@cam.ac.uk

Conflict of interest disclosures: No author has any to declare.

Word Count: 3770

Number of Figures: 5

Number of Tables: 3

## **Abstract**

**Objective** Traumatic brain injury (TBI) is not a single insult with monophasic resolution, but a chronic disease, with dynamic processes that remain active for years. We aimed to assess patient trajectories over the entire disease narrative, from ictus to late outcome.

**Methods** Twelve patients with moderate-to-severe TBI underwent magnetic resonance imaging in the acute phase (within 1 week of injury) and twice in the chronic phase of injury (median 7 and 21 months), with some undergoing imaging at up to two additional time points. Longitudinal imaging changes were assessed using structural volumetry, deterministic tractography, voxel based diffusion tensor analysis, and region of interest analyses (including corpus callosum, parasagittal white matter, and thalamus). Imaging changes were related to behaviour.

**Results** Changes in structural volumes, fractional anisotropy, and mean diffusivity continued for months to years post-ictus. Changes in diffusion tensor imaging were driven by alterations in both axial and radial diffusivity, and were associated with changes in reaction time and performance in a visual memory and learning task, (paired associates learning). Dynamic structural changes after TBI can be detected using diffusion tensor imaging and could explain changes in behaviour.

**Conclusions.** These data can provide further insight into early and late pathophysiology, and begin to provide a framework that allows magnetic resonance imaging to be used as an imaging biomarker of therapy response. Knowledge of the temporal pattern of changes in TBI patient populations also provides a contextual framework for assessing imaging changes in individuals at any given time point.

## Introduction

Despite being precipitated by an acute event, it is becoming clear that traumatic brain injury (TBI) is not a single insult with monophasic resolution, but a chronic disease, with dynamic processes that remain active for years.<sup>1</sup> Both the acute illness and dynamic change over time result in physical and neuropsychological problems, which represent a substantial burden on the individual and society. Although ameliorating these deficits would be of substantial benefit, the mechanisms that underlie them are poorly characterised.

One of the most promising techniques to provide a means of addressing the neuroanatomical substrate of such disease evolution is diffusion tensor imaging (DTI).<sup>2,3</sup> This technique characterises the diffusion of water molecules in tissue environments, which are influenced by the microstructural organization of tissues and their constituent cells, and can provide unique insights into pathophysiology, particularly in white matter (WM).

Previous studies in TBI have typically found consistent reductions in fractional anisotropy (FA) in classical areas affected by traumatic axonal injury (TAI), even when conventional magnetic resonance imaging showed no lesion.<sup>4-9</sup> There is some evidence of dynamic white matter change over a longer time period.<sup>10,11</sup> Both of these studies found that most change (especially in the corpus callosum (CC)) occurred between their first (approximately 1 to 2 months), and second (approximately 1 to 2 years) time points. This temporal framework of comparing imaging within weeks of injury with repeat

imaging only at chronic time points (months to years) is a disadvantage where imaging changes are being used to interrogate processes involved in either progressive pathology or repair, since the resolution of oedema in the first few weeks after TBI introduces an important confound, which dominates imaging changes. Early after an injury oedema may be associated with an increase in diffusivity (vasogenic oedema) and/or restricted diffusivity (cytotoxic oedema).<sup>12</sup> Such pathology will also lead to changes with the diffusion tensor influencing the calculated fractional anisotropy and making early tractography difficult a reduction in of fibres may be secondary to oedema rather than true track loss.

In order to gain insight into the microstructural substrates of late recovery or progressive deterioration the dynamic evolution of pathology from the acute to the post-acute phase after TBI needs to be examined. Our aims in this study were: to use DTI fully characterise the entire narrative of disease between hours and years following TBI; to identify the microstructural substrates for both late recovery and deterioration in individual patients; and to undertake correlations between imaging findings and performance on a canonical neurobehavioral task, using targeted behavioural metrics with well-established neuroanatomical substrates.

## Methods

Twelve patients underwent serial imaging using a 3 Tesla Siemens Magnetom TIM Trio at a minimum of three and up to five times after injury (see Table 1 for timing details). No patients had a history of previous TBI. All scans within the first three weeks were performed while patients required sedation and ventilation. There were no major scanner upgrades during the duration of the study. Ethical approval was obtained from the Local Research Ethics Committee (LREC 97/290) and written consent was obtained.

The imaging protocol included DTI (12 non-collinear directions, 6 b values equally spaced between 0 and 1588 s/mm<sup>2</sup>, 2mm isotropic voxels, repetition time = 8300ms, echo time = 98ms) and a 3D T1-weighted structural sequence (MPRAGE, isotropic voxel size of 1x1x1mm). Imaging data was also collected in 30 age and gender matched controls, of which a subset of eight subjects underwent three sessions over an 18 month period.

Neuropsychological testing was performed on patients on the same day as the imaging session for all time points in and beyond the sixth month after injury. Tests, designed to test memory, executive function and attention were selected from the CANTAB battery of tests (Table 2, [www.cambridgecognition.com](http://www.cambridgecognition.com)).

## **Structural volumetric analysis**

The T1-weighted images were preprocessed using the N4 algorithm to correct for intensity inhomogeneities.<sup>13</sup> The images were extracted with a brain mask calculated with pinfram (<http://www.soundray.org/pinfram/>). A multi-atlas segmentation approach based on manually segmented brains from the OASIS database was used to segment the images (<http://Neuromorphometrics.com>).<sup>14</sup> Registration was performed using MAPER, an approach which incorporates tissue probability maps into the registration and relies on a non-rigid registration based on free-form deformations.<sup>15,16</sup> Using symmetric intra-subject registration<sup>17,18</sup> temporally corresponding scans were aligned. In an expectation-maximization framework the availability of probabilistic segmentation estimates were exploited to perform a symmetric intensity normalization and segmentation. Symmetric differential bias correction for images in presence of pathologies was performed. A consistent multi-time-point segmentation was achieved using a spatially and temporally varying Markov random field.<sup>19</sup> Volumetric analysis was performed in two canonical regions that have been strongly correlated with injury mechanisms and sites that impact on TBI outcome; whole brain white matter (WBWM) and the thalami.

## **Diffusion tensor imaging analyses**

### **Tractography**

Whole brain deterministic tractography was performed for all patient scans and the larger set of controls to provide a representation of the overall atrophy of the WM. Streamline tractography was performed in the native diffusion space based on the Euler

Delta Crossings algorithm using Diffusion Imaging in Python software (<http://dipy.org>) and the number of these “tracks” quantified.<sup>20</sup> Ten thousand seed points were used with a FA threshold of 0.2.

## **Region of interest analysis**

FMRIB’s Diffusion Toolbox (FDT) was used to create FA, MD and eigenvalue maps (<http://www.fmrib.ox.ac.uk/fsl>). To aid coregistration, the skull, and extracranial soft tissue were stripped from the MPRAGE images using the Brain Extraction Tool.<sup>21</sup> Region of interest (ROI) analysis was performed in the anterior CC, chosen as being representative of WM damage from TAI, and the thalamus as being, an important grey matter (GM) region affected in TBI. No significant differences in any diffusivity values were found between the right and left thalamic regions of interest (data not shown, available on request) and so for ease of assessment they were combined in this analysis. Regions were manually drawn on the T1 weighted image in MNI space using Analyze 7.0 (<http://www.mayo.edu/bir>). ROIs were transformed to the native diffusion space of patients using the vtkCISG mutual information algorithm.<sup>16</sup> Mean FA, MD and eigenvalues for each ROI were obtained.

## **Voxel-based analysis of DTI**

Although some studies have use tract based spatial statistics (TBSS) to quantify white matter changes after TBI,<sup>22,23</sup> we chose to use tensor based morphometry (TBM) analysis to address the hypothesis that that WM injury would not be restricted to the centre of major tracts but would also affect more peripheral WM, as well as the GM. FA

maps were coregistered to MNI152 space and averaged to create a customized template.<sup>16</sup> FA and MD maps were coregistered to this study specific template and smoothed with a 10mm isotropic Gaussian kernel.

To ascertain which areas of the brain were affected by longitudinal change after TBI, a flexible factorial model (allowing for unequal variances) was implemented in subjects who had an acute (the patient's first scan, median 31, range 14 to 44 hours), subacute (median 40, range 29 to 86 days) and chronic scans (the patient's last scan, median 422, range 358 to 949 days). These three time points were chosen *a priori*, as it was hypothesised that the largest changes would be observed between these time points. The model included eight controls that had undergone three imaging sessions.

To examine whether change in cognitive and motor performance was related to changes in imaging parameters, change in FA and MD was correlated with changes in performance in two canonical tasks (simple reaction time, and an index of memory function as measured by a paired associates learning task (PAL)). These tasks were chosen these based on their relevance to TBI. Motor slowing is a pervasive finding in this patient group,<sup>24,25</sup> and the PAL, a visuospatial associative learning task sensitive to mild cognitive impairment, has previously been shown in a cross-sectional analysis to correlate with diffusivity parameters after chronic TBI.<sup>25,26</sup> Differences in performance metrics between the two time points were calculated for each subject, as were difference maps in FA and MD for the same interval. Correlations between change maps and changes in test scores were assessed using linear regression

([www.fil.ion.ucl.ac.uk/spm/software/spm8](http://www.fil.ion.ucl.ac.uk/spm/software/spm8)), where changes in test scores were independent variables and change maps were the dependent variables. To increase sensitivity, all correlations of neuropsychological variables were limited to the WM for FA correlations and to GM for MD correlations. For all TBM correction for multiple comparisons was based on the family-wise error rate ( $p < 0.05$ ).<sup>27</sup> To create scatter plots relating the change in FA and MD to change in reaction time, the significant regions were extracted and applied to the FA and MD change maps to obtain the individual patient values.

## Statistical analyses

Except for the TBM, statistical analyses were conducted using SPSS (SPSS 18.0, Chicago, IL, USA, <http://www.spss.com>). Mann-Whitney U was used for unpaired tests and the Wilcoxon signed rank test for paired comparisons.  $p \leq 0.05$  was accepted as significant.

In order to assess whether there was a significant correlation between the time to scan and either the change in volume of neuroanatomical structures or the number of tracks quantified, the data were fitted to a general linear model. All patients and time points were included in this analysis. The different subjects were modelled as a fixed factor and the time to scan was included as a covariate. The interaction between subjects and time since injury was also considered:

$$\text{data} = \beta_0 + \beta_1 * (\text{subject}) + \beta_2 * (\text{time since injury}) + \beta_3 * (\text{subject} \times \text{time since injury}) + \varepsilon$$

## Results

The patients' median (range) admission Glasgow Coma Score was 5 (3 to 11) and Glasgow Outcome Score was 4 (3 to 5) (Table 1). The median time to scan one was 33 (range 16 to 190) hours, scan two 165 (68 to 395) hours, scan three 40 days (range 29 to 86 days), scan four 225 days (range 147 to 534 days), and scan five 651 days (range 358 to 1015 days).

**Table 1:** Demographic and clinical characteristics of the patients. All patients were imaged in the acute phase (within 1 week of injury) and twice at least 5 months after injury. Eight patients had a second imaging session while still inpatient in the critical care unit and seven had an imaging session in the subacute phase of injury (more than 21 days after injury when it would be expected that oedema has resolved) at a median of 40 days after injury.

Patient	Age at injury (years)	Gender	Cause of Injury	GCS	MARSHALL Score	ISS	APACHE	Days in ICU	GOSE	Scan 1 Acute (hours)	Scan 2 Acute (hours)	Scan 3 subacute (days)	Scan 4 Chronic 1 (days)	Scan 5 Chronic 2 (days)
1	17.4	M	RTC	6	DI II	29	15	23	8	20	134	63	223	412
2	20.7	M	RTC	8	DI II	18	22	19	5	16	137		391	756
3	17.3	F	RTC	3	DI II	20	21	26	8	41		86	261	949
4	46.8	F	RTC	5	DI II	25	21	18	6	35	221	29	199	409
5	21.6	M	RTC	3	EML	43	36	7	4	31		47	198	863
6	59.2	M	Fall	4	DI II	26	21	12	6	20	68	31	181	358
7	17.5	M	RTC	3	DI II	25	23	20	8	190			257	810
8	25.4	M	RTC	7	DI II	26	16	5	6	20	188		147	677
9	49.5	F	Fall	5	EML	17	22	23	6	14	230	37	174	607
10	22.1	F	RTC	11	Vic	9	15	12	6	109	396		268	396
11	50.5	M	RTC	10	DI II	9	19	7	6	44			534	1015
12	32.0	M	RTC	3	DI III	38	28	8	5	44	142	40	220	422

GCS = post-resuscitation GCS<sup>28</sup>; M = male, F = female, RTC – road traffic collision. Marshall Grade<sup>29</sup> = scored on initial CT. I to IV = diffuse injury, V = evacuated mass lesion, VI = non evacuated mass lesion; ISS = Injury Severity Score, higher scores indicate greater severity<sup>30</sup>; APACHE = Acute Physiology and Chronic Health Evaluation, higher scores indicate greater severity<sup>31</sup>; 6 month GOSE = Glasgow Outcome Score – Extended;<sup>32</sup> 1 = death, 2= vegetative state, 3 = low severe disability, 4 = upper severe disability, 5 = low moderate disability, 6 = upper moderate disability, 7 = low good recovery, 8 = upper good recovery.

At the time of first neurocognitive testing (scan four) performance on spatial working memory was no different to controls (Table 2). In contrast, significant differences were found in all or some components of reaction time, rapid visual information processing, pattern recognition, spatial recognition, PAL and spatial span. Between the two neurocognitive testing sessions, for the group as a whole, there were significant improvements in reaction time, rapid visual information processing A', spatial recognition and PAL.

**Table 2:** Summary of the results of the neuropsychological tests used. Values shown are median(interquartile range) for non-parametric data ( \* P < 0.05, \*\* p < 0.01, \*\*\* p < 0.001).

Tasks	Task Summary	Task Variables	Controls	TBI Scan 4 Chronic 1	Scan 5 Chronic 2	Controls Vs Scan 4	Controls Vs Scan 5	Scan 4 Vs Scan 5
<b><u>Attention</u></b>								
Simple Reaction Time	Assesses reaction time	Latency (ms)	709 (604 to 783)	876 (734 to 1078)	743 (620 to 823)	0.025*	0.722	0.019*
Rapid Visual Information Processing	A test of sustained attention that also requires working memory. The aim is to detect infrequent three-digit sequences from among serially presented digits.	A'	0.93 (0.88 to 0.96)	0.84 (0.81 to 0.89)	0.89 (0.83 to 0.92)	0.002**	0.035*	0.013*
		B'	0.96 (0.90 to 1.00)	0.93 (0.90 to 0.97)	0.97 (0.90 to 1.00)	0.346	0.631	0.169
		Latency (ms)	404 (389 to 429)	523 (457 to 590)	365 (347 to 428)	0.001**	0.063	0.005**
<b><u>Visual memory</u></b>								
Pattern Recognition	A two-choice test of abstract visual pattern recognition memory.	Percentage correct	95.8 (93.8 to 100)	85.4 (80.2 to 91.7)	85.4 (83.3 to 92.7)	0.011*	0.029*	0.528
		Latency (ms)	1667 (1413 to 2077)	2355 (1741 to 2843)	1889 (1550 to 2310)	0.030*	0.436	0.047*
Spatial Recognition	Two-choice forced discrimination paradigm to test spatial recognition memory.	Percentage correct	87.5 (83.8 to 90.0)	75.0 (66.3 to 83.8)	85.4 (7.8 to 91.3)	0.009**	0.853	0.024*
		Latency (ms)	1804 (1376 to 2392)	2095 (1891 to 2964)	2165 (1794 to 2492)	0.203	0.529	0.333
Paired Associate Visual Learning	A test of the ability to form visuo-spatial associations.	Errors at 6 box (adjusted)	0 (0 to 2.3)	6.50 (3.3 to 10.8)	4.0 (0 to 6.0)	0.000***	0.072	0.018*

<b><u>Executive Function, working memory and planning</u></b>								
Spatial Working Memory	A test of spatial working memory and strategy performance to find individually hidden "blue tokens" without returning to a box where one has previously been found.	<p><b>Within errors</b> Returning to a box that has already been inspected.</p> <p><b>Strategy</b> Reflects the consistency of the search sequencing.</p> <p><b>Between errors</b> Returning to a box where a token has been found.</p>	0 (0 to 0.25)	0 (0 to 4)	0 (0 to 1.5)	0.254	0.631	0.891
			10.0 (1.0 to 18.5)	22.0 (7.8 to 39.5)	8.0 (4.0 to 8.)	0.095	0.905	0.153
			25.0 (21.0 to 35.3)	33.0 (28.3 to 34.8)	30.5 (20.8 to 37.3)	0.254	0.579	0.593
Intra-dimensional/Extra-dimensional (ED) Shift	Test of visual discrimination learning which assesses the ability to selectively attend to and shift between a number of stimulus dimensions, including shape and colour.	<b>Stages completed</b>	9.0 (9.0 to 9.0)	9 (7.5 to 9)	9.0 (9.0 to 9.0)	0.582	1.00	0.317
Spatial span	A test of the subject's ability to recall the order in which a series of boxes were highlighted.	<b>Span length</b>	7.5 (6.0 to 8.0)	6.0 (5.0 to 6.75)	6.0 (5.8 to 8.0)	0.030*	0.436	0.054

## **Structural Volumetric Analysis**

The volumes calculated at each time point for the patients can be seen in Figure 2 for the thalamus and WBWM. The percentage change in volume over 18 months (Tables 3 and 4) for controls was significantly less than the patients (Median (IQR): Thalamus; -0.66 (-2.01 to 1.81),  $p < 0.001$ ; WBWM; -0.17 (-0.74 to 0.44),  $p < 0.001$ ). There was significant negative correlation with time to scan for the WBWM (F-value = 605,  $p$ -value  $< 0.001$ ), thalami (F-value = 627,  $p$ -value  $< 0.001$ ) and whole brain volume (F-value = 143,  $p$ -value  $< 0.001$ ) consistent with atrophy over time.

**Table 3:** Percentage change in thalamic volume between each scan for the patients.

Patient	Scan 2 – Scan 1	Scan 3 – Scan 2	Scan 4 – Scan 3	Scan 5 – Scan 3	Scan 5 – Scan 4	Scan 5 – Scan 1
1	7.8	-24.0	6.4	3.6	-2.6	-15.2
2	2.9				-7.0	-16.3
3			-0.7	-4.0	-3.3	-10.0
4	-2.6	-6.8	-3.2	-6.7	-3.7	-15.4
5			-7.7	-26.5	-20.4	-33.6
6	0.8	-8.3	-0.1	-1.3	-1.2	-8.8
7					1.7	-4.1
8	0.5				-4.0	-12.4
9	-2.7	-10.9	6.8	4.6	-2.1	-9.3
10	-17.7				1.1	-6.9
11					-0.8	-9.0
12	0.1	-6.3	7.4	0.3	-6.7	-5.0
<b>Median</b>	0.3	-8.3	-0.1	-1.3	-3.0	-9.7
<b>(IQR)</b>	(-2.6 to 2.4)	(-17.5 to -6.6)	(-3.2 to 6.8)	(-6.7 to 3.6)	(-6.0 to -0.9)	(-15.3 to -7.4)

**Table 4:** Percentage change in whole brain white matter volume between each scan for the patients.

Patient	Scan 2 – Scan 1	Scan 3 – Scan 2	Scan 4 – Scan 3	Scan 5 – Scan 3	Scan 5 – Scan 4	Scan 5 – Scan 1
1	-0.1	-8.8	-3.2	-3.9	-7.0	-15.3
2	2.0			-12.8		-20.2
3			-5.4	-0.8	-6.1	-23.8
4	1.2	-9.9	-3.0	-4.0	-6.9	-15.0
5			1.6	1.4	3.0	-0.1
6	-1.2	-4.9	-3.9	-2.1	-5.9	-11.5
7				-1.3		-11.0
8	13.9			-2.0		-14.3
9	4.4	-10.3	-3.2	-2.6	-5.7	-11.7
10	0.6			-0.1		-15.4
11				-0.6		-4.5
12	1.9	-12.7	-2.8	-4.5	-7.1	-17.5
<b>Median</b>	1.5	-9.9	-3.2	-2.0	-6.1	-14.6
<b>(IQR)</b>	(0.1 to 3.8)	(-11.5 to -6.8)	(-3.9 to -2.8)	(-4.0 to -0.6)	(-7.0 to -5.7)	(-16.9 to -11.2)

## **Diffusion Tensor Imaging Analysis**

### **Tractography Analysis**

Qualitative inspection of the streamline tractography images showed WM loss in all patients with TBI, which was widespread in the supratentorial compartment, but also involved the cerebellum and brainstem (Figure 1). The temporal progression of these changes varied between patients, with some patients showing gradual recovery of WM tracts following acute injury, whereas others showed a progressive loss of WM.

Quantitative assessment of fibre counts in individual patients confirmed this variation between patients (Figure 2). The generalised linear model analysis found that both time to scan (F-value = 12.68, p-value = 0.002) and the interaction between subject and time to scan (F-value = 4.20, p-value = 0.002) was significant, consistent with different patient trajectories.

### **Region of interest analysis**

In the eight controls scanned over time FA and MD in both the CC and thalamic ROIs showed no significant change. In a group analysis comparing all patients with the larger control group, FA in the CC was significantly lower in patients than in controls at second acute (scan 2), subacute (scan 3) and first chronic scan (scan 4) ( $p < 0.05$ , Mann-Whitney U) (Figure 3, Table 2). An inspection of temporal patterns showed that FA appeared to continue to decrease from the first scan to a nadir at scan 4 (first chronic scan). The CC FA in patient regions of interest was not significantly different from the control group at the second chronic scan (scan 5). The MD in the CC was

significantly lower than control values in the first scan after injury, but increased to control or supra-control levels at subsequent time points. The changes in FA and MD were driven by a decrease in the axial and radial diffusivities at the most acute time point. For all subsequent time points FA reduction was driven by increases in the axial and disproportionately larger increases in radial diffusivities. In contrast the thalamic region of interest showed a transient significant increase in FA and decrease in MD in the first acute scan (Figure 3, Table 2), but subsequently showed reduced FA and increased MD by scan 5.

### **Voxel based diffusion tensor analysis**

The FA factorial analysis of DTI images over time in the control and patient groups revealed a group by time interaction. Regions which showed significant changes over time in the TBI cohort on serial FA maps included the anterior and posterior CC, the parasagittal WM, and frontal and posterior WM (Figure 4). Significant changes on MD maps in the TBI cohort included the thalamus and grey-white matter junctions. Changes in FA and MD over serial images were driven by alterations in both axial and radial diffusivity.

### **Neuropsychological correlations with DTI**

Contemporaneous measures of cognitive and motor performance were available for time points four and five. Significant correlations were found between change in reaction time with change in FA in the anterior and posterior WM, anterior CC, and the anterior limb of the internal capsule (Figure 5A). Improvements in reaction time were

associated with an increase in FA in these regions. In contrast, a reduction in thalamic MD on serial assessment was associated with improvements in reaction time. These correlations were most prominent in the ventral tegmentum and anterior cingulate cortex (Figure 5A). There were no significant associations showing a positive correlation with FA or negative correlation with MD. The correlation for the change for regions identified in Figure 5A versus change in reaction time were; FA ( $r = -0.601$ ,  $p = 0.039$ ) and MD ( $r = 0.790$ ,  $p = 0.002$ ).

Figure 5B shows the association between changes in performance on PAL (measured as errors at six boxes) with serial changes in FA and MD. Decrements in PAL performance correlated with reductions in FA in the anterior limb of the internal capsule (bilaterally) and the frontal WM, predominantly on the right ( $r = -0.814$ ,  $p < 0.014$  for the composite region of interest). Decrements in PAL performance correlated with increases in MD, predominantly in the right insula ( $r = 0.898$ ,  $p < 0.002$ ).

While most patients showed improvements (defined as moving towards control values) in DTI metrics between these two late time points (increases in FA and reductions in MD), some patients showed continued deterioration (further reductions when compared to control values in FA and increases in MD). Critically, for both tasks in patients when DTI metrics moved towards control values they were associated with improvements in performance and deterioration in DTI metrics further away from control values were associated with worsening in cognate tasks.

## Discussion

This study provides compelling evidence of dynamic changes after moderate to severe TBI, which continue into the subacute and chronic phases after TBI. We believe that our study is the first to provide data at multiple time points, ranging over the entire disease narrative, ranging from the hyperacute phase through to chronic follow up. Critically, we also show that these changes in structure may relate to changes in function.

The exact time course, relative importance and trajectory of each pathophysiological process after TBI is still open to great debate. Indeed, given the heterogeneity seen in TBI, there are likely to be different inter-individual differences between patients and within the patients at different time points. In addition, multiple mechanisms may underlie the imaging changes observed, further complicating the assessment and interpretation of findings. Given this background, it is critical to specify a temporal context for imaging changes, since the same imaging finding may have very different meaning and significance at different points, and even at the same time point but different location (for example in GM and WM).<sup>33</sup>

Both the initial injury and second insults (such as hypoxia, hypotension and raised intracranial pressure) trigger a complex array of microscopic and microstructural changes, including cytotoxic oedema, astrocyte swelling, microglial activation and vasogenic oedema.<sup>34</sup> Animal studies indicate that diffusivity parameters change rapidly in the first hours to days after injury,<sup>35</sup> a finding replicated in the changes between our

earliest scan (median 33 hours) and the second scan (median 165 hours) (Figure 4). Animal studies implicate early cytotoxic oedema as a driver for these rapid changes, which include a transient early increase in FA in GM regions<sup>35</sup> (as seen in our thalamic ROI). This is consistent with early human ischemic stroke where a transient increase in FA has been found in the first 4.5 hours after ischemic stroke.<sup>36</sup> The disproportionate increase found in radial diffusivity in the second acute scan leading to an increase in MD and reduction in FA is consistent with worsening (likely) vasogenic oedema. The rapidity of such changes underlines the need to precisely account for time after injury in group analyses in imaging studies of TBI. By four weeks after injury many of the acute processes, including oedema, are likely to have largely resolved, even in those patients with raised intracranial pressure in the acute phase.

Changes in diffusivity parameters in chronic TBI have been shown to correlate with outcome at specific time points.<sup>37</sup> However, changes occurring in the later stages of TBI are likely to be the result of a complex interplay of many processes. Wallerian degeneration and demyelination, can occur (for example) in thalamic projection fibres,<sup>38</sup> and progress for several months.<sup>39</sup> Neuronal loss, particularly in the frontal cortex (shown with histopathology)<sup>40</sup> and thalamus (as illustrated using <sup>11</sup>C-flumazenil positron emission tomography)<sup>41</sup> correlate with outcome. TBI also appears to trigger a long-term inflammatory response, with microglial activation in areas remote to the original site of injury.<sup>24</sup> Histopathological evidence of gliosis has been associated with an increase in FA in the GM and decrease in the WM in a rat model.<sup>42</sup> Finally, both adaptive and maladaptive plasticity may also occur, and studies in status epilepticus suggest that FA

increases in the dentate gyrus of the rat hippocampus may be the imaging correlate of an increase in density of myelinated fibers and mossy fibre sprouting.<sup>43</sup>

In clinical studies, maximal behavioural recovery occurs in the early months after injury with a plateau at six to eighteen months. Longer term studies suggest that patients continue to evolve for years after injury. Whitnall et al reported that when survivors were assessed five to seven years after injury, 29% had improved and 25% deteriorated when compared to assessments performed one year after injury.<sup>28</sup> The fact that patients may improve, stay the same, get progressively worse, or decline after many years of stability indicate a complex interplay of factors, and it is likely that adaptive and maladaptive processes are occurring in parallel. The pattern and heterogeneity of dynamic changes in our study is consistent with the clinical patterns of recovery reported by Whitnall et al.<sup>28</sup>

Our data replicate the large decreases in brain volume reported in earlier studies (8.4% at 2 months and a further 4% by a year),<sup>44</sup> which far exceed that seen in healthy controls (who show no loss between 18 and 35, and annual brain volume losses of 0.5% after age 60).<sup>45</sup> However, the ability to trace trajectories of regional volume change from the initial phase of acute oedema offers additional insights, by demonstrating different regional vulnerabilities and trajectories of atrophy in response to injury.

Whole brain tractography has the advantage of requiring no a priori selection of specific tracks, and so may provide a picture of the overall burden of WM loss, and by implication, of connectivity in the injured brain. However, it is important to note that the path counts from such analyses are not a true reflection of the actual fibre number but instead represent a measure of the relative anatomical integrity of fibres. The decrease in paths counted may reflect microstructural changes in the cortex, including the loss of fibres or demyelination, either of which could lead to consequent axonal and tract dysfunction and cognitive sequelae. Future studies with higher angular resolution data could further subdivide tracks to see whether particular pathways have a predilection for damage after TBI and correlate with functional status.

DTI has been used in cross-sectional analyses to study neurocognitive function in TBI with varying success, and performance in specific cognitive areas (executive function, memory and attention),<sup>6</sup> evoked motor responses,<sup>46</sup> and decision making<sup>37</sup> have been shown to correlate with the burden of WM injury in select areas. Farbota and colleagues were able to show that changes in DTI metrics were related to performance on serial neuropsychological measures but were unable to isolate such coordinated change in imaging and behavioural measures to the first or second imaging intervals.<sup>11</sup> Further, their analysis was limited to the supratentorial WM, and could simply reflect the overall severity of traumatic axonal injury (TAI), rather than representing specific neuroanatomical substrates for cognate cognitive deficits. It is also not possible from their analyses to determine whether the relationship between DTI and

behavioural change was bidirectional (i.e. showing concordance for both improvement and deterioration). Our data suggest that DTI might provide a biomarker of both recovery and progression of pathophysiology. The specificity of the correlations between individual behavioural metrics and their cognate neuroanatomical substrates raise the possibility that we may be able to use these approaches to selectively address neuroanatomical change relevant to target cognitive processes. We recognised that inclusion of acute imaging data in correlational analyses may have provided an artifactual confound due to inappropriate dependence on the acute data, where oedema was a prominent pathophysiological process. Consequently, the correlations that we present between behaviour and imaging only reflect imaging data obtained at late points at which such behavioural assessment was possible, and make no use of data obtained at early time points.

The PAL is sensitive to mild cognitive impairment in TBI.<sup>25</sup> Previous work by our group correlated increased errors on this task with increased diffusivity in neural areas known to be important in this task, including the hippocampal formation, frontal and temporal cortices.<sup>26</sup> In other studies, performance on memory tasks in patients a year after mild TBI was found to correlate with the uncinate fasciculus.<sup>7</sup> The cross-sectional correlations between patients in these past studies are now replicated in the temporal associations we show within patients, in the form of correlations between performance on the PAL and imaging changes in left parasagittal and left frontal WM and right insula GM (Figure 5).

Our study has clear limitations which need to be acknowledged. Some of these limitations are dictated by our clinical substrate. Imaging patients, particularly those at the severe end of the TBI spectrum, presents significant challenges. At early stages patients may be sedated and mechanically ventilated, making scanning sessions long and complex. During the early recovery period, patients may be agitated and find it difficult to lie still in the scanner. Challenges like these mean that the exact timing of scans in this study varies between patients, and in the case of the two chronic scans means there is some overlap. As a consequence, where possible, the actual scan date has been used as a variable. This was not possible for the flexible factorial model in the voxel based diffusion tensor analysis. However, longitudinal studies with larger numbers of patients, and more tightly defined time points, are required to more completely understand the temporal trajectory of TBI. Additional imaging studies with other modalities will be required to confirm some of the mechanistic inferences that we hypothesise, such as the use of [ $^{11}\text{C}$ ]flumazenil positron emission tomography for selective neuronal loss, [ $^{11}\text{C}$ ]PK11195 positron emission tomography for microglial activation, and functional MRI to map the functional consequences of structural abnormalities that we demonstrate.

## **Conclusions**

Our assessment of longitudinal changes in diffusivity parameters at multiple time points, and correlation of these changes with dynamic changes in function has allowed improved characterisation of the spectrum and behavioural associations of temporal changes in TBI. These data may enhance outcome evaluation, and help provide a

mechanistic basis for deficits that remain unexplained by other approaches. Such knowledge of longitudinal patterns of change in patient populations is important to aid interpretation of imaging findings in individuals. Future studies with larger numbers of patients will help provide further insight into late pathophysiology, help select appropriate patients for clinical trials, and provide a framework that allows MRI to be used as an imaging biomarker of therapy response.

## **Funding**

This work was supported by a Medical Research Council (UK) Program Grant (Acute brain injury: heterogeneity of mechanisms, therapeutic targets and outcome effects [G9439390 ID 65883]), the UK National Institute of Health Research Biomedical Research Centre at Cambridge, and the Technology Platform funding provided by the UK Department of Health. VFJN is supported by a Health Foundation/Academy of Medical Sciences Clinician Scientist Fellowship. TG was supported by the Société Française d'Anesthésie et de Réanimation (SFAR). PJAH is supported by a National Institute for Health Research Professorship. DKM is supported by an NIHR Senior Investigator Award and by an FP7 grant from the European Commission. The funders had no role in study design, data collection and analyses, decision to publish, or preparation of the manuscript.

## Figure Legends

**Figure 1:** Whole brain diffusion tensor tractography in an age-matched control subject and two patients with serial images at approximately two days, six weeks, and one year following severe traumatic brain injury. The series of images for the first patient shows gradual temporal recovery of white matter integrity in traumatic brain injury, with continuing incremental change between weeks and months post-traumatic brain injury. In the second patient such recovery does not occur; in contrast, there appears to be continuing and progressive white matter loss weeks to months post-injury. Tracks that run superiorly/inferiorly are blue, anterior/posterior green and left/right red.

**Figure 2:** Individual patient trajectories for thalamic volume, whole brain white matter volume and whole brain tractography in control subjects and patients post severe traumatic brain injury longitudinally. Dashed lines have been superimposed on the figure to show continuity of subjects between the acute phase (shown in hours) and the more chronic phases of recovery (shown in days). The shaded areas indicate the range for controls.

**Figure 3:** Trends over time for fractional anisotropy (FA), mean diffusivity (MD), axial and radial diffusivity for the anterior corpus callosum (top) and thalamic (bottom) regions of interest. The central lines in the boxes denote the median values, the upper and lower edges the 75<sup>th</sup> and 25<sup>th</sup> percentiles, the error bars the 90<sup>th</sup> and 10<sup>th</sup> percentiles, and closed circles the data outside these percentiles.

**Figure 4:** Changes over time in FA, MD, axial and radial diffusivity. FA changes (orange) are mainly confined to the white matter including the anterior and posterior corpus callosum, the parasagittal white matter, frontal and posterior white matter. MD changes (blue) occur mainly in the grey matter including the thalamus and grey-white matter junctions. Axial diffusion (red) and radial diffusion (green) follow a similar pattern to the MD. For all voxel based diffusion tensor analyses correction for multiple comparisons was based on the family-wise error rate ( $p < 0.05$ ).

**Figure 5:** Change in cognitive function is significantly correlated with change in cerebral microstructure in patients over the early chronic phase of traumatic brain injury. Panel A shows the association of diffusion imaging parameters with reaction time. Negative correlation with FA is shown in orange/yellow indicating a faster reaction time with an increase in FA. Positive correlation with the MD is shown in blue indicating a faster reaction time with a decrease in ADC. There were no significant association with a positive correlation with FA or negative correlation with MD. Panel B shows how performance on the paired associates learning task correlated with FA in the white matter (orange/yellow) and MD in the grey matter (blue). Only a negative correlation was found with FA indicating more errors were associated with lower FA in the left

parasagittal white matter, anterior limb/genu of the internal capsule (bilateral) and frontal white matter (left > right). For MD only a positive correlation was found concentrated in the right insula. Panels C and D show scatterplots of change in diffusion imaging parameters for significant brain regions in Panel A with change in reaction time (Spearman's Rho; Graph C: MD ( $r = 0.790$ ,  $p = 0.002$ ), Graph D: FA ( $r = -0.601$ ,  $p = 0.039$ )). In patients where the imaging parameters moved closer to those of controls their reaction time tended to improve, with the converse for those whose imaging parameters worsened.

## References

1. Walker KR, Tesco G. Molecular mechanisms of cognitive dysfunction following traumatic brain injury. *Frontiers in aging neuroscience*. 2013;5:29.
2. Basser PJ, Pierpaoli C. Microstructural and physiological features of tissues elucidated by quantitative-diffusion-tensor MRI. *Journal of magnetic resonance. Series B*. Jun 1996;111(3):209-219.
3. Hulkower MB, Poliak DB, Rosenbaum SB, Zimmerman ME, Lipton ML. A decade of DTI in traumatic brain injury: 10 years and 100 articles later. *AJNR. American journal of neuroradiology*. Nov-Dec 2013;34(11):2064-2074.
4. Bendlin BB, Ries ML, Lazar M, et al. Longitudinal changes in patients with traumatic brain injury assessed with diffusion-tensor and volumetric imaging. *Neuroimage*. Aug 15 2008;42(2):503-514.
5. Greenberg G, Mikulis DJ, Ng K, DeSouza D, Green RE. Use of diffusion tensor imaging to examine subacute white matter injury progression in moderate to severe traumatic brain injury. *Archives of physical medicine and rehabilitation*. Dec 2008;89(12 Suppl):S45-50.
6. Kraus MF, Susmaras T, Caughlin BP, Walker CJ, Sweeney JA, Little DM. White matter integrity and cognition in chronic traumatic brain injury: a diffusion tensor imaging study. *Brain*. 2007;130(Pt 10):2508-2519.
7. Niogi SN, Mukherjee P, Ghajar J, et al. Extent of microstructural white matter injury in postconcussive syndrome correlates with impaired cognitive reaction time: a 3T diffusion tensor imaging study of mild traumatic brain injury. *AJNR. American journal of neuroradiology*. May 2008;29(5):967-973.
8. Rutgers DR, Toulgoat F, Cazejust J, Fillard P, Lasjaunias P, Ducreux D. White matter abnormalities in mild traumatic brain injury: a diffusion tensor imaging study. *AJNR. American journal of neuroradiology*. Mar 2008;29(3):514-519.
9. Sidaros A, Engberg AW, Sidaros K, et al. Diffusion tensor imaging during recovery from severe traumatic brain injury and relation to clinical outcome: a longitudinal study. *Brain*. Feb 2007;131(Pt 2):559-572.
10. Dinkel J, Drier A, Khalilzadeh O, et al. Long-Term White Matter Changes after Severe Traumatic Brain Injury: A 5-Year Prospective Cohort. *AJNR. American journal of neuroradiology*. Dec 12 2013.
11. Farbota KD, Bendlin BB, Alexander AL, Rowley HA, Dempsey RJ, Johnson SC. Longitudinal diffusion tensor imaging and neuropsychological correlates in traumatic brain injury patients. *Frontiers in human neuroscience*. 2012;6:160.
12. Newcombe VF, Williams GB, Outtrim JG, et al. Microstructural basis of contusion expansion in traumatic brain injury: insights from diffusion tensor imaging. *Journal of cerebral blood flow and metabolism : official journal of the International Society of Cerebral Blood Flow and Metabolism*. Jun 2013;33(6):855-862.
13. Tustison NJ, Avants BB, Cook PA, et al. N4ITK: improved N3 bias correction. *IEEE transactions on medical imaging*. Jun 2010;29(6):1310-1320.
14. Marcus DS, Wang TH, Parker J, Csernansky JG, Morris JC, Buckner RL. Open Access Series of Imaging Studies (OASIS): cross-sectional MRI data in young, middle aged, nondemented, and demented older adults. *Journal of cognitive neuroscience*. Sep 2007;19(9):1498-1507.
15. Modat M, Ridgway GR, Taylor ZA, et al. Fast free-form deformation using graphics processing units. *Computer methods and programs in biomedicine*. Jun 2010;98(3):278-284.

16. Rueckert D, Sonoda LI, Hayes C, Hill DL, Leach MO, Hawkes DJ. Nonrigid registration using free-form deformations: application to breast MR images. *IEEE transactions on medical imaging*. Aug 1999;18(8):712-721.
17. Leung KK, Ridgway GR, Ourselin S, Fox NC, Alzheimer's Disease Neuroimaging I. Consistent multi-time-point brain atrophy estimation from the boundary shift integral. *Neuroimage*. Feb 15 2012;59(4):3995-4005.
18. Ledig C, Shi W, Makropoulos A, et al. Consistent and robust 4D whole-brain segmentation: application to traumatic brain injury. *IEEE 11th International Symposium on Biomedical Imaging*. 2014.
19. Ledig C, Heckemann RA, Hammers A, et al. Robust whole-brain segmentation: application to traumatic brain injury. *Medical Imaging Analysis*. In Press.
20. Garyfallidis E, Brett M, Correia MM, Williams GB, Nimmo-Smith I. QuickBundles, a method for tractography simplification. *Frontiers in Brain Imaging Methods*. 2012;6(175).
21. Chen XH, Johnson VE, Uryu K, Trojanowski JQ, Smith DH. A lack of amyloid beta plaques despite persistent accumulation of amyloid beta in axons of long-term survivors of traumatic brain injury. *Brain Pathol*. Apr 2009;19(2):214-223.
22. Hellyer PJ, Leech R, Ham TE, Bonnelle V, Sharp DJ. Individual prediction of white matter injury following traumatic brain injury. *Annals of neurology*. Nov 29 2012.
23. Spitz G, Maller JJ, O'Sullivan R, Ponsford JL. White matter integrity following traumatic brain injury: the association with severity of injury and cognitive functioning. *Brain topography*. Oct 2013;26(4):648-660.
24. Ramlackhansingh AF, Brooks DJ, Greenwood RJ, et al. Inflammation after trauma: microglial activation and traumatic brain injury. *Annals of neurology*. Sep 2011;70(3):374-383.
25. Salmond CH, Chatfield DA, Menon DK, Pickard JD, Sahakian BJ. Cognitive sequelae of head injury: involvement of basal forebrain and associated structures. *Brain : a journal of neurology*. Jan 2005;128(Pt 1):189-200.
26. Salmond CH, Menon DK, Chatfield DA, et al. Diffusion tensor imaging in chronic head injury survivors: correlations with learning and memory indices. *NeuroImage*. Jan 1 2006;29(1):117-124.
27. Worsley KJ, Marrett S, Neelin P, Vandal AC, Friston KJ, Evans AC. A unified statistical approach for determining significant signals in images of cerebral activation. *Hum Brain Mapp*. 1996;4(1):58-73.
28. Whitnall L, McMillan TM, Murray GD, Teasdale GM. Disability in young people and adults after head injury: 5-7 year follow up of a prospective cohort study. *J Neurol Neurosurg Psychiatry*. May 2006;77(5):640-645.
29. Marshall LF, Marshall SB, Klauber MR, et al. The diagnosis of head injury requires a classification based on computed axial tomography. *J Neurotrauma*. Mar 1992;9 Suppl 1:S287-292.
30. Greenspan L, McLellan BA, Greig H. Abbreviated Injury Scale and Injury Severity Score: a scoring chart. *J Trauma*. Jan 1985;25(1):60-64.
31. Wagner DP, Draper EA, Abizanda Campos R, et al. Initial international use of APACHE. An acute severity of disease measure. *Med Decis Making*. 1984;4(3):297-313.
32. Jennett B, Bond M. Assessment of outcome after severe brain damage. *Lancet*. Mar 1 1975;1(7905):480-484.
33. Newcombe VF, Williams GB, Nortje J, et al. Concordant biology underlies discordant imaging findings: diffusivity behaves differently in grey and white matter post acute neurotrauma. *Acta neurochirurgica. Supplement*. 2008;102:247-251.

34. Buki A, Povlishock JT. All roads lead to disconnection?--Traumatic axonal injury revisited. *Acta Neurochir (Wien)*. Feb 2006;148(2):181-193; discussion 193-184.
35. Mac Donald CL, Dikranian K, Song SK, Bayly PV, Holtzman DM, Brody DL. Detection of traumatic axonal injury with diffusion tensor imaging in a mouse model of traumatic brain injury. *Experimental neurology*. May 2007;205(1):116-131.
36. Puig J, Blasco G, Daunis IEJ, et al. Increased corticospinal tract fractional anisotropy can discriminate stroke onset within the first 4.5 hours. *Stroke; a journal of cerebral circulation*. Apr 2013;44(4):1162-1165.
37. Newcombe V, Chatfield D, Outtrim J, et al. Mapping traumatic axonal injury using diffusion tensor imaging: correlations with functional outcome. *PLoS one*. 2011;6(5):e19214.
38. Little DM, Kraus MF, Joseph J, et al. Thalamic integrity underlies executive dysfunction in traumatic brain injury. *Neurology*. 2010;74(7):558-565.
39. Wilson S, Raghupathi R, Saatman KE, MacKinnon MA, McIntosh TK, Graham DI. Continued in situ DNA fragmentation of microglia/macrophages in white matter weeks and months after traumatic brain injury. *J Neurotrauma*. Mar 2004;21(3):239-250.
40. Maxwell WL, MacKinnon MA, Stewart JE, Graham DI. Stereology of cerebral cortex after traumatic brain injury matched to the Glasgow outcome score. *Brain*. 2010;133(Pt 1):139-160.
41. Kawai N, Maeda Y, Kudomi N, Yamamoto Y, Nishiyama Y, Tamiya T. Focal neuronal damage in patients with neuropsychological impairment after diffuse traumatic brain injury: evaluation using (1)(1)C-flumazenil positron emission tomography with statistical image analysis. *J Neurotrauma*. Dec 2010;27(12):2131-2138.
42. Budde MD, Janes L, Gold E, Turtzo LC, Frank JA. The contribution of gliosis to diffusion tensor anisotropy and tractography following traumatic brain injury: validation in the rat using Fourier analysis of stained tissue sections. *Brain*. Aug 2011;134(Pt 8):2248-2260.
43. Laitinen T, Sierra A, Pitkanen A, Grohn O. Diffusion tensor MRI of axonal plasticity in the rat hippocampus. *Neuroimage*. Jun 2010;51(2):521-530.
44. Sidaros A, Skimminge A, Liptrot MG, et al. Long-term global and regional brain volume changes following severe traumatic brain injury: a longitudinal study with clinical correlates. *Neuroimage*. Jan 1 2009;44(1):1-8.
45. Hedman AM, van Haren NE, Schnack HG, Kahn RS, Hulshoff Pol HE. Human brain changes across the life span: a review of 56 longitudinal magnetic resonance imaging studies. *Hum Brain Mapp*. Aug 2012;33(8):1987-2002.
46. Nakayama N, Okumura A, Shinoda J, et al. Evidence for white matter disruption in traumatic brain injury without macroscopic lesions. *J Neurol Neurosurg Psychiatry*. Jul 2006;77(7):850-855.

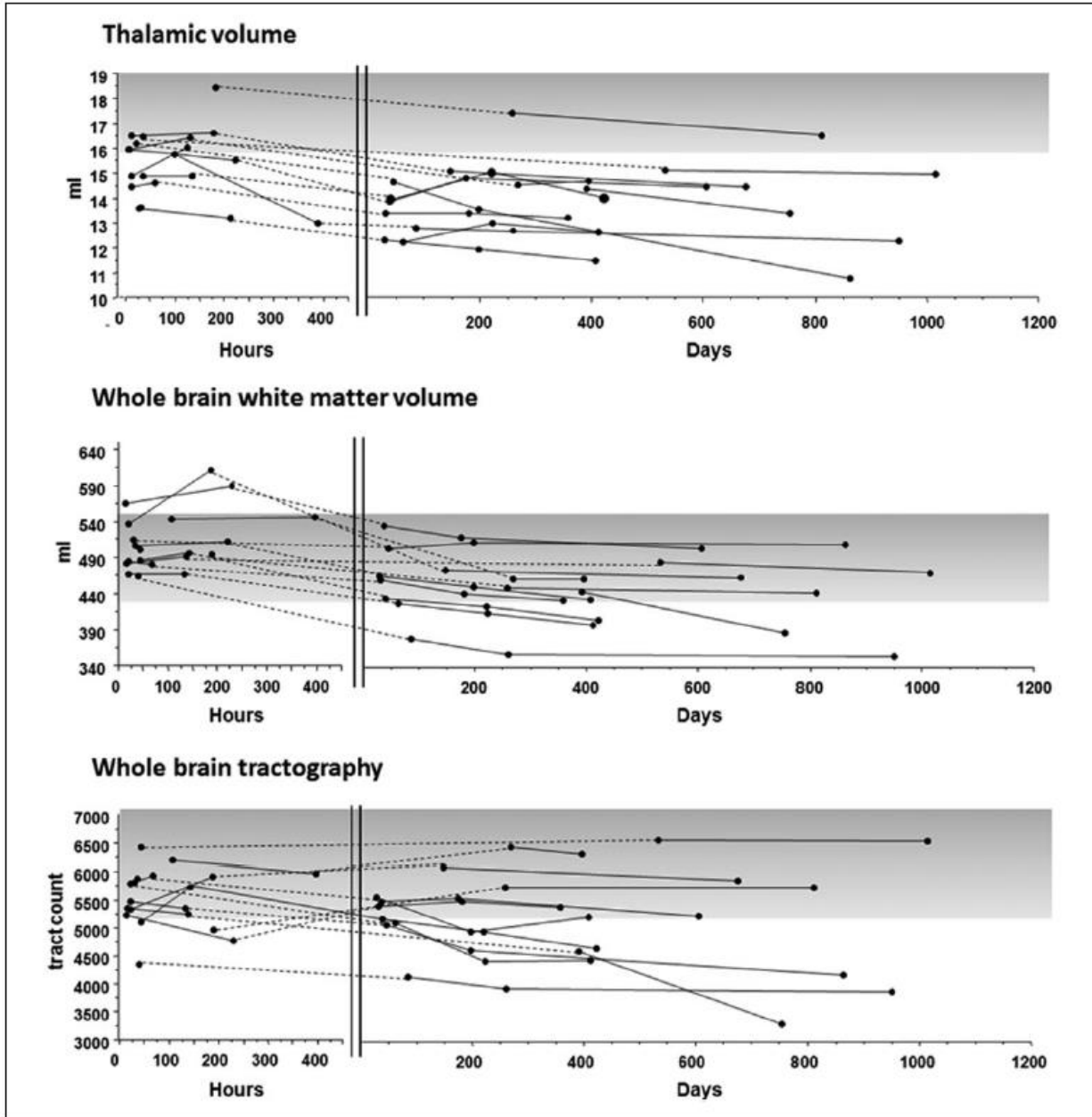


Figure 1

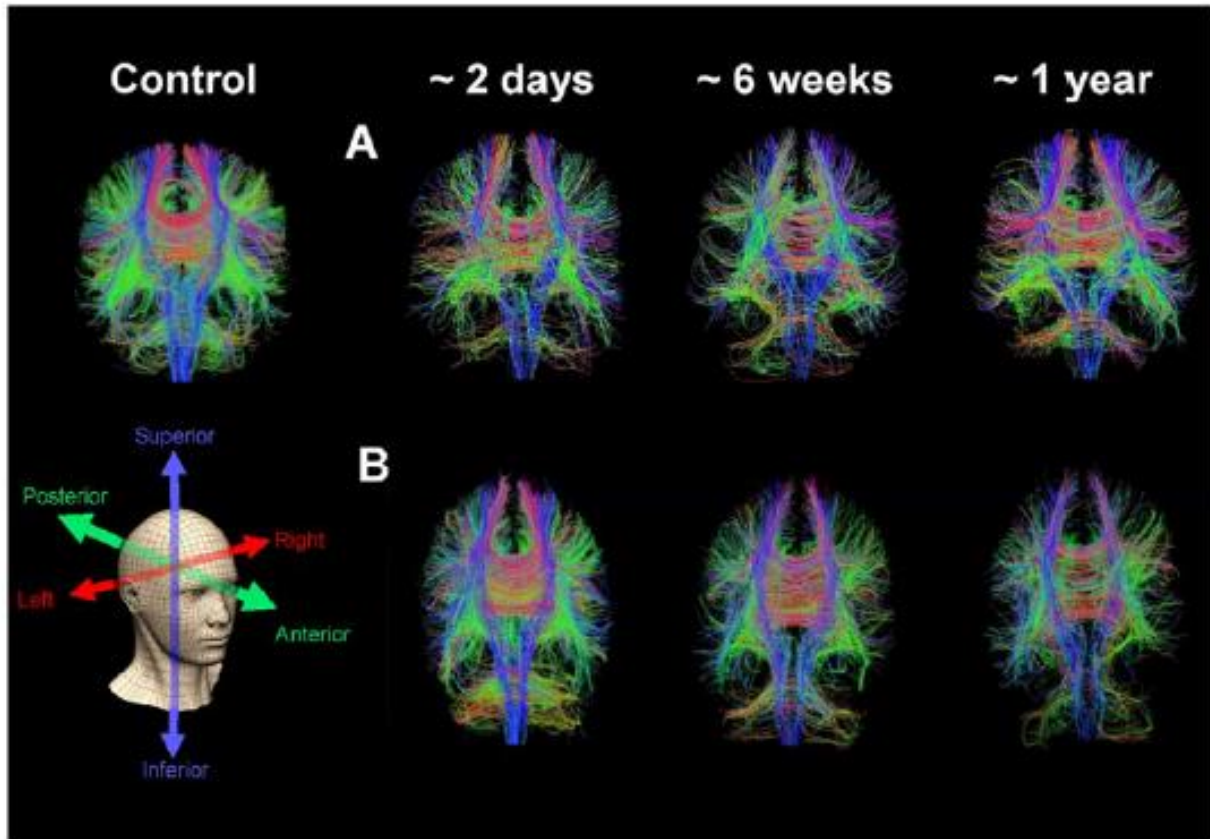


Figure 2

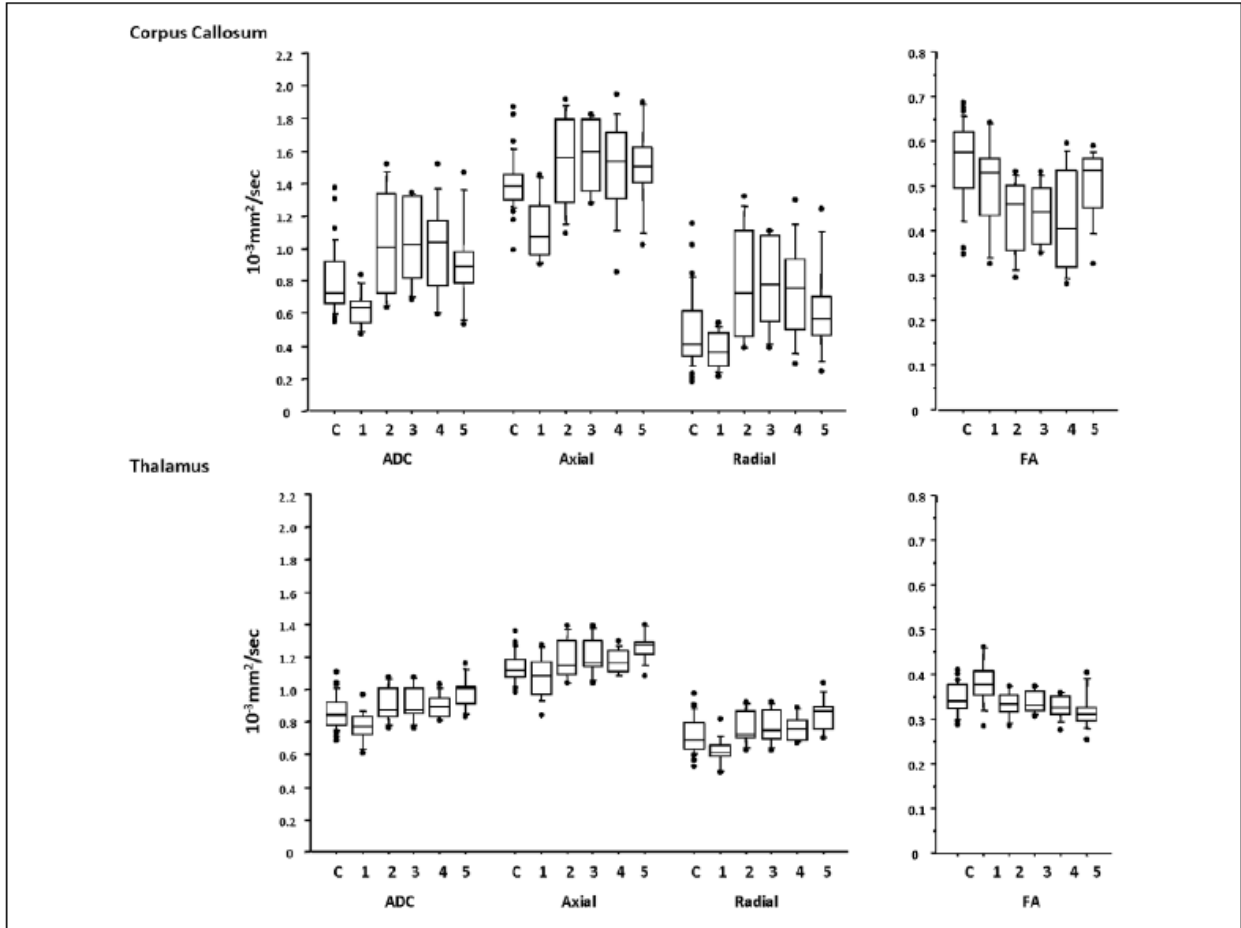


Figure 3

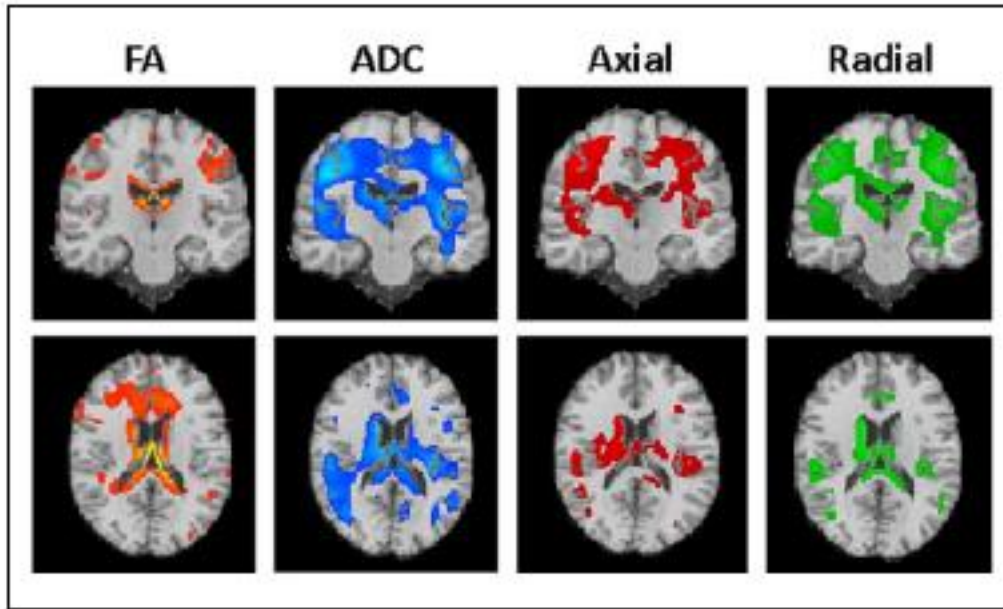


Figure 4

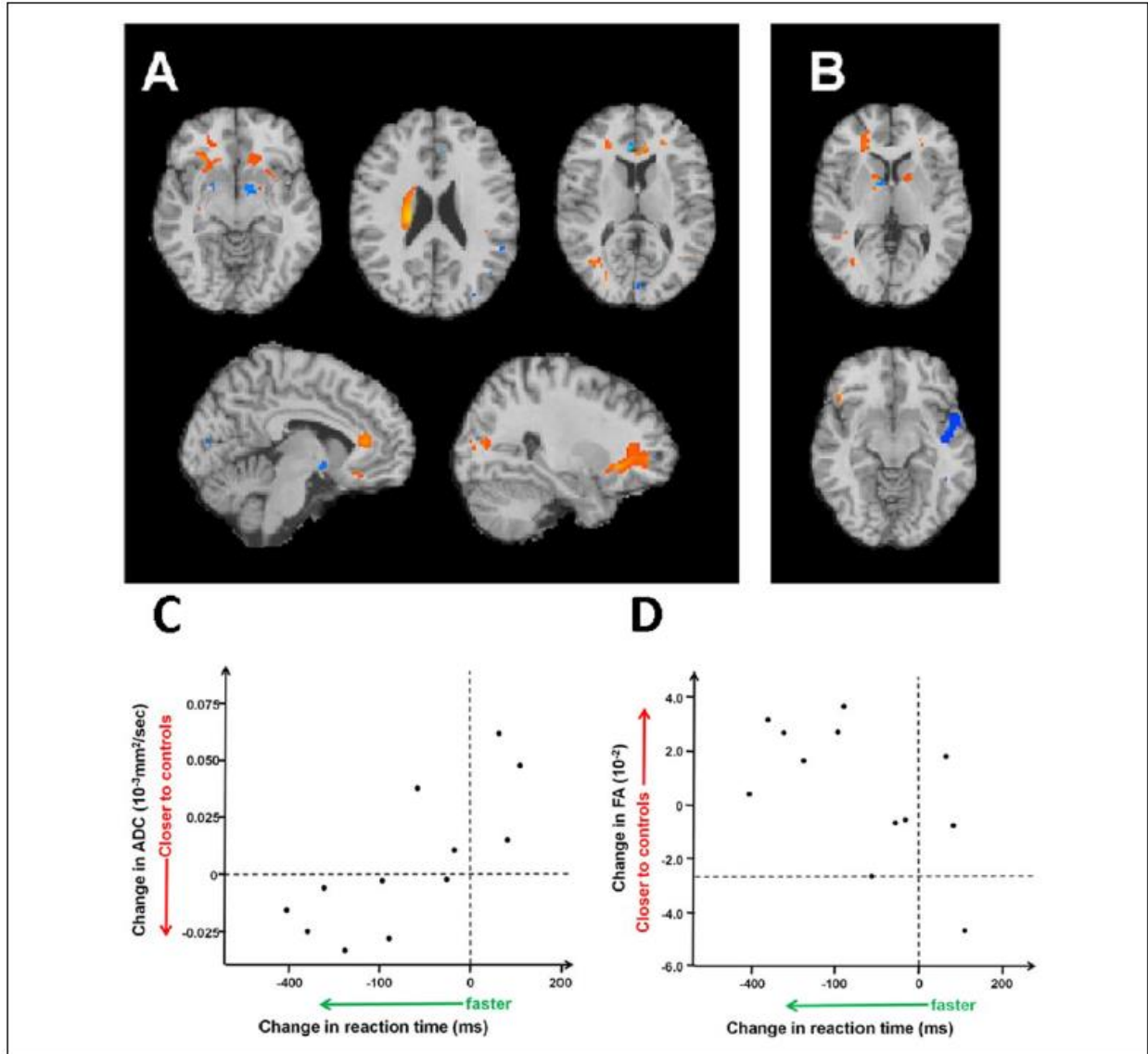


Figure 5